Square-Planar Cobalt(II)

DOI: 10.1002/anie.201311183

Two-Orbital Three-Electron Stabilizing Interaction for Direct Co^{2+}–As^{3+} Bonds involving Square-Planar CoO_4 in $BaCoAs_2O_5$**

*Rénald David, Houria Kabbour, Alain Pautrat, Nadia Touati, Myung-Hwan Whangbo, and Olivier Mentré**

Abstract: *The quest for new oxides with cations containing active lone-pair electrons (E) covers a broad field of targeted specificities owing to asymmetric electronic distribution and their particular band structure. Herein, we show that the novel compound $BaCoAs_2O_5$, with lone-pair As^{3+} ions, is built from rare square-planar $Co^{2+}O_4$ involved in direct bonding between $As^{3+}E$ and Co^{2+} d_{z2} orbitals (Co–As = 2.51 Å). By means of DFT and Hückel calculations, we show that this σ-type overlapping is stabilized by a two-orbital three-electron interaction allowed by the high-spin character of the Co^{2+} ions. The negligible experimental spin-orbit coupling is expected from the resulting molecular orbital scheme in O_3AsE–CoO_4 clusters.*

Transition-metal oxides containing lone pair (LP) cations exhibit fascinating properties. In oxides consisting of post-transition-metal cations (e.g., Pb^{2+}, Bi^{3+}) with LPs, the filled s orbital of the cation interacts with the filled p orbitals of its surrounding anions (e.g., O^{2-}) leading to antibonding states with a high degree of cation s character, which contribute strongly to the valence band top. The mixing of the empty p orbitals of the cation (e.g., $6s^26p^0$ for Bi^{3+}) into these antibonding states, which is enhanced by an asymmetric distortion around the cation, forms the LP of the cation.[1,2] Systems with such a cation LP orbital cover a broad range of interesting materials, which include photocatalysts with optical transitions involving the LP states at the top of the valence bands (e.g., $BiVO_4$,[3] Bi_2WO_6),[4] multiferroics based on the pyramidal inversion of the cation with LP (e.g., perovskites $BiMnO_3$, and $BiFeO_3$)[5] and low-band-gap transparent conducting materials with hole conduction, (e.g. good *p*-type mobilities in SnO and PbO[2]). In cases where the presence of LP electrons on a given element needs to be emphasized, the symbol *E* will be added.

Neutral and anionic species with LPs (e.g., phosphine EPX_3, arsine $EAsX_3$ (X = H, halogen, R, and others) are commonly-encountered two-electron donor ligands in organometallic compounds.[6] In contrast, it is very rare that LP-containing cations bond directly to transition-metal cations as ligands. A few examples known so far involve the As^{3+} ions of pyramidal $EAsO_3$ groups, which are bonded to Cu^+ (d^{10}) ions to form tetrahedral clusters with short Cu–As bonds, and to low-spin Fe^{2+} (d^6) ions to form octahedral clusters with short As–Fe bonds; such as the tetrahedral $CuAs_4$ cluster of dixenite with As–Cu = 2.240 (×3) and 2.336 (×1) Å,[7] the tetrahedral $CuAs_2Cl_2$ cluster of freedite with Cu–As = 2.32 Å,[8] and the tetrahedral $CuCl_3As$ cluster of $Pb_6Cu(AsO_3)_2Cl_7$ with As–Cu = 2.34 Å.[9] In the octahedral $FeAs_6$ clusters of nanlingite,[10] the low-spin Fe^{2+} (d^6) ion is surrounded by six As^{3+} ions with As-Fe = 2.40 Å. While exploring systems containing cobalt and arsenic in reducing media, we prepared the new phase $BaCoAs_2O_5$ in which nearly square-planar CoO_4 units containing Co^{2+} ions interact with $EAsO_3$ pyramids containing As^{3+} ions to form CoO_4As square pyramids with short Co^{2+}–As^{3+} bonds (2.51 Å), as compared to those mediated by oxygen atoms commonly found in oxides. We show that this As–Co bond is stabilized because the interaction between the filled d_{z2} Co^{2+} orbital and the LP of As^{3+} becomes a two-orbital three-electron stabilizing interaction due to the high-spin character of the Co^{2+} ion.

$BaCoAs_2O_5$ crystallizes in the space group $P2_1/m$, with lattice parameters $a = 7.2151(4)$ Å, $b = 5.4504(3)$ Å, $c = 7.2816(4)$ Å and $\beta = 104.2960(3)°$. It has $(CoAs_2O_5)_2$ slabs alternating with layers of Ba^{2+} ions (Figure 1a) along the *a* direction. Each slab has two $(CoAs_2O_5)$ layers made up of As_2O_5 groups and nearly square-planar CoO_4 units (Co-O =

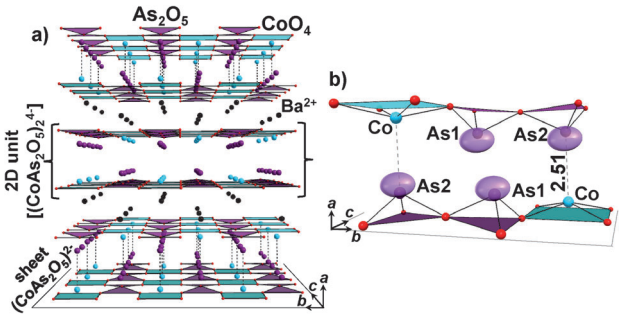

Figure 1. a) Structure of $BaCoAs_2O_5$. b) The interaction between a lone pair and a Co atom.

[*] R. David, H. Kabbour, O. Mentré
Université Lille Nord de France, CNRS UMR8181, Unité de Catalyse et de Chimie du Solide, UCCS USTL
59655 Villeneuve d'Ascq (France)
E-mail: olivier.mentre@ensc-lille.fr
A. Pautrat
CRISMAT, UMR 6508-CNRS, ENSICAEN, Caen (France)
N. Touati
LASIR, UMR 8516, USTL, Villeneuve d'Ascq (France)
M.-H. Whangbo
Department of Chemistry, North Carolina State University (USA)

[**] R.D. thanks the ENS of Lyon for financial support. This work was carried out under the framework of the ANION-CO project supported by the ANR (Grant ANR-12-JS08-0012).

Supporting information for this article is available on the WWW under http://dx.doi.org/10.1002/anie.201311183.

2.014–2.028 Å) sharing their oxygen corners. Each CoO_4 unit has the Co^{2+} ion shifted vertically out of the O_4 plane by 0.44 Å, but will be referred to as square-planar CoO_4 hereafter, for simplicity. Each As_2O_5 group consists of $As1O_3$ and $As2O_3$ pyramids sharing an oxygen corner with their two As^{3+} LPs present on one side of the As_2O_5 basal plane. In $(CoAs_2O_5)_2$ slabs, the two $CoAs_2O_5$ layers are stacked such that the CoO_4 square planes on one layer make short Co^{2+}–$As2^{3+}$ bonds (2.51 Å) with the As^{3+} ions on the other layer (see Figure 1b), whereas the As1 atoms do not make such bonds.

The direct Co^{2+}–As^{3+} bond of the O_3As–CoO_4 unit is surprising because the Co^{2+} ion in the square-planar CoO_4 has a doubly filled d_{z^2} orbital, which would have a σ-type overlap with the doubly-filled E orbital of the next As^{3+}, giving rise to strong two-orbital four-electron destabilization.[11] To gain insight into this puzzling feature, we carried out extended Hückel tight-binding calculations[12,13] for isolated CoO_4 and O_3As–CoO_4 units. Our results are summarized in Figure 2,

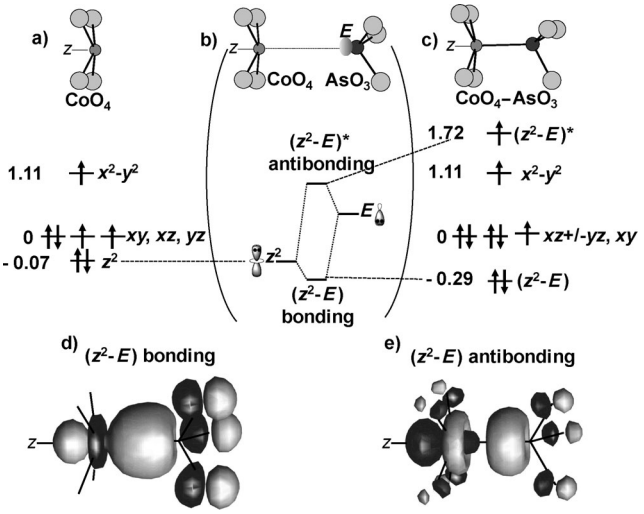

Figure 2. EHTB molecular orbitals for a) CoO_4 and c) CoO_4–AsO_3. b) Creation of (z^2-E) and (z^2-E)* by two-orbital σ interaction. Energy levels are given in eV.

where it is assumed that the Co^{2+} (d^7) ion is in the high-spin state (see below for further discussion). For the CoO_4 unit, the d levels are split as $d_{z2} < d_{xy}$,(d_{xz}, d_{yz}) < d_{x2-y2}. The d_{xy} level is nearly degenerate with the degenerate (d_{xz}, d_{yz}) level, because the Co^{2+} ion is shifted from the O_4 plane.[11] For the O_3As–CoO_4 unit, the interaction of the d_{z2} of CoO_4 with the LP electrons (E) of AsO_3 leads to the σ-bonding level (z^2-E) and the σ antibonding level (z^2-E)*, leading to the orbital sequence (z^2-E) < d_{xy},(d_{xz}, d_{yz}) < d_{x2-y2} < (z^2-E)*. The (z^2-E) level lies lower in energy than the d_{z2} of the CoO_4 unit by $\Delta E = -0.22$ eV. Given the high-spin state of the Co^{2+} ion, the (z^2-E) level is doubly occupied, but the (z^2-E)* level is singly occupied. Therefore, the interaction between the d_{z2} orbital of Co^{2+} and the LP electrons of As^{3+} becomes a two-orbital three-electron stabilizing interaction.[11] The (z^2-E) level has a stronger contribution from the As^{3+} level E than does the d_{z2} level of CoO_4, and hence can be regarded as the stabilized lone-pair level of As^{3+}. Then, the (z^2-E)* level is the d_{z2} level destabilized by the As^{3+} level E. Our density functional theory (DFT) calculations (see below), carried out for the ferromagnetic state of $BaCoAs_2O_5$ for simplicity, are in support of the above analysis. The calculations show a magnetic moment of about 2.6 μB from GGA + U, with $U = 3$ eV, on a Co^{2+} ion and a band gap of about 2.07 eV. The projected density of states (PDOS) plots, presented in Figure 3, show an

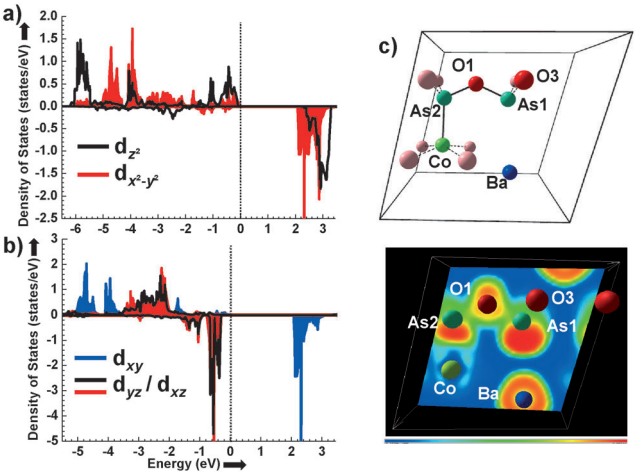

Figure 3. The spin-polarized projected DOS from GGA + U calculations ($U = 3$ eV) for the d states of Co: a) $d_{x^2-y^2}$ and d_{z^2} states, and b) d_{xy}, d_{xz}, d_{yz} states. The dotted lines indicate the Fermi levels. c) Slice of the valence ELF of $BaCoAs_2O_5$. Blue corresponds to almost no electron localization and orange to complete localization.

exchange splitting between the majority (up spin) and minority (down spin) Co 3d states expected for a high-spin Co^{2+} ion; the d_{xz} and d_{yz} are doubly filled, while the d_{xy}, d_{z2} and d_{x2-y2} levels are singly filled in agreement with the Co^{2+} ion high-spin state (d^7, $S = 3/2$).

The square-planar coordination of cobalt in the O_3As–CoO_4 unit is rare in inorganic compounds. The known examples are $A_2Cu_2Co^{2+}O_2S_2$ (A = Ba, Sr)[14] and $Sr_2Co^{2+}O_2X_2$ (X = Cl, Br),[15] which contain axially-elongated $Co^{2+}O_4L_2$ octahedra (L = S, X) with long Co–L bonds (Co–S = 3.37 Å in the former[16] and Co–Cl = 2.745 Å in the latter).[15] For a series of compounds with various axial Co–L or Co–O lengths, the experimental ordered-moment (μ_T) of the Co^{2+} ion (i.e., the sum of the spin and orbital moments ($\mu_S + \mu_L$) was found to increase as the bond-length ratio (r = Co–L/Co–O) increased.[16] For an ion with more than a half-filled d shell such as Co^{2+} (d^7), μ_S and μ_L have the same sign,[17,18] so that the above observation indicates that μ_L, which results from spin orbit coupling (SOC), mimics the r variation. For the axially-elongated CoO_4L_2 octahedron, the d orbitals of the high-spin Co^{2+} ion split, with $(d_{z2})^2 < (d_{xz}, d_{yz})^3 < (d_{xy})^1 < (d_{x2-y2})^1$. The SOC of the filled down-spin $(d_{z2})^2$ level with the empty down-spin of one of the (d_{xz}, d_{yz}) levels is possible because their L_z values differ by one (i.e., $\Delta L_z = \pm 1$), and the energy lowering is inversely proportional to the energy difference (Δe) between the d_{z2} and (d_{xz}, d_{yz}) levels.[11,18] As Δe decreases with increasing r, the SOC, and

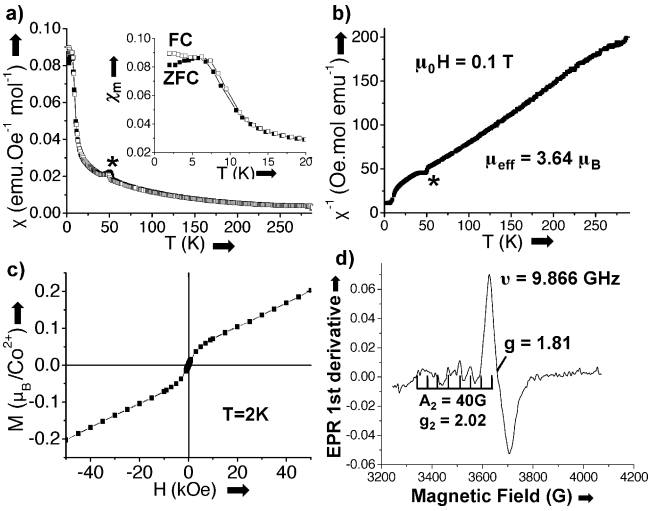

Figure 4. Magnetic/EPR characterizations of $BaCoAs_2O_5$: a) $\chi(T)$ plot at 0.01T with ZFC/FC divergence in the inset. b) $\chi^{-1}(T)$ plot at 0.1 T. An asterisk (*) indicates an anomaly due to O_2 solidification. c) M(H) curve at 2 K. d) EPR X-band spectrum at room temperature

hence the μ_L value, increases with increasing *r*. In $BaCoAs_2O_5$ (Figure 3a) the filled down-spin $(d_{xz}, d_{yz})^4$ levels can engage in SOC with the empty down-spin $(d_{z2})^1$ level. However, Δe is large (1.72 eV), so that the effect of the SOC may be very weak. We verified this assessment by performing X-band EPR measurements at room temperature (9.866 GHz frequency) on $BaCoAs_2O_5$. Despite abundant literature on HS–Co^{2+} EPR spectroscopy,[19,20] the unusual Co coordination (*Cs* symmetry with a Co–As direct interaction on one side) found in $BaCoAs_2O_5$ was not theoretically investigated to our knowledge. According to the Co coordination, we can expect $g_x \approx g_y \neq g_z$. The spectrum shows a main resonance at $g_1 = 1.92$, which was assigned to g_x/g_y because of its intensity. A badly resolved multiplet structure at $g_2 = g_z = 2.02$ was also detected (partially overlapping with the former; Figure 4a). The latter eight lines would correspond to a ($S = 3/2$, $I = 7/2$) hyperfine coupling with the splitting parameter $A_2 = 40$G. The absence of any other absorption band was checked. This feature reasonably suggests a nearly isotropic $g \approx 2$ Landé factor. Magnetic susceptibility measurements on $BaCoAs_2O_5$ (Figure 4a) also confirm the absence of significant SOC, because the effective paramagnetic moment $\mu_{eff} = 3.64\ \mu_B$ is very close to the spin-only value of $3.72\ \mu_B$ using the experimental *g* value. Then, the weak SOC of the Co^{2+} ion in $BaCoAs_2O_5$ is similar to those found in La_2CoO_4,[21] $La_2Co_2O_5$,[22] and $La_4Co_3O_9$,[23] the low μL values of which are also believed to arise from the high-lying empty down-spin d_{z2} level.[16]

The Curie–Weiss temperature of $BaCoAs_2O_5$ is $\theta_{CW} = -32$ K, which indicates the presence of dominant antiferromagnetic exchange. The zero-field-cooled (ZFC) and field-cooled (FC) susceptibilities diverge below 8 K (Figure 4a) when the system antiferromagnetically orders. The magnetization M(H) curves (Figure 4b) show the existence of a weak net moment above $H_c = 5$ KOe, possibly owing to spin canting. Finally, according to the weak magnetization values ($M = 0.2\ \mu_B$ at μ_0. $H = 5$ T), it can be concluded that antiferromagnetic exchanges take place in the ($CoAs_2O_5$) layers, which are comparatively stronger than those found for other similarly layered $Ba^{2+}/Co^{2+}/(As^{5+},As^{3+})/O^{2-}$ systems that undergo spin-flip transitions under an external magnetic field.[24,25]

The bond valence sums (BVSs) of the As and Co atoms calculated by using the parameters of Brese and O'Keeffe[26] are summarized in Table 1. The As2 atom engaged in the Co–As bond formation has a larger BVS than does the As1 atom (+3.44 vs. +3.23), suggesting that the participation into the two-orbital three-electron interaction leads to a more electropositive As^{3+} center and hence shorter As–O bonds. The BVS of Co^{2+} is calculated to be smaller than +2 (i.e., +1.67) by considering only the Co–O bonds. To come up with the BVS of +2 for Co^{2+}, the Co–As bond should contribute the BVS of +0.33. On the basis of the BVS formula, $s = \exp[(r_0 - r)/B)]$ with $s = 0.33$, $B = 0.37$ and $r = 2.51$ Å, we derive $r_0 = 2.13$ for the Co^{2+}–As^{3+} bond. A similar value of $r_0 = 1.99$ was extracted for the Fe^{2+}–As^{3+} bond from the $FeAs_6$ octahedra in nanlingite.[10]

Table 1: Wyckoff positions, atomic coordinates, and thermal parameters for $BaCoAs_2O_5$.

Atom	Wyck	*x*	*y*	*z*	Ueq. [Å²]
Ba1	2d	0.9229(1)	0.25	0.7287(1)	0.010(1)
As1	2d	0.3609(1)	0.25	0.5661(1)	0.009(1)
As2	2d	0.3549(1)	0.25	0.1093(1)	0.008(1)
Co	2d	0.2863(1)	−0.25	0.8180(1)	0.010(1)
O1	2d	0.2496(6)	0.25	0.3104(7)	0.013(1)
O2	4d	0.7740(5)	−0.0043(6)	0.0019(4)	0.012(1)
O3	4d	0.2251(5)	0.0051(6)	0.6117(5)	0.013(1)

Distances [Å]

Atom	$d_{X\text{-}As2}$	$d_{X\text{-}O2}$	$d_{X\text{-}O3}$	$d_{X\text{-}O4}$	BV
Ba1		2×2.844(3)	2×2.860(4)	2×2.980(3)	2.07
		2×2.882(3)	2×2.813(3)		
As1			2×1.736(4)	1.837(5)	3.23
As2		2×1.716(3)		1.808(5)	3.44
Co	2.510(5)	2×2.028(3)	2×2.014(3)		1.67

The electron localization function (ELF) allows the visualization of the nodal structure of the molecular orbital, including LP electrons.[27] Figure 2c shows a cross-sectional view of the ELF on the Co–As1–As2 plane, where the electrons associated with As1 and As2 (the orange and red lobes, respectively) pointing away from their oxygen neighbors. The LP stereochemistry can be visualized on both As1 and As2 from the ELF, as it appears lobe-shaped whereas the Ba atoms show a spherical localization in agreement with its ionic character in the structure.

Finally, we probe the point that, in oxides of post-transition-metal elements with LP-bearing cations, the top portion of their valence bands has contributions from the cation ns, the cation np, and the oxygen 2p orbitals.[1] We find that this picture remains valid for $BaCoAs_2O_5$ by calculating the PDOS plots for the O 2p, As 4s and As 4p states, as shown in Figure S1 of the Supporting Information. The As 4s states are present at the top portion of the valence band (−2 to 0 eV

region), as well as around −6 eV, as expected from Figure 2. In the same energy regions, the contributions of the O 2p and As 4p states also occur, as expected.

In summary, we have synthesized the new phase $BaCoAs_2O_5$ by hydrothermal synthesis in reducing hydrazonium media. It has Co atoms in square-pyramidal CoO_4As units with a short Co^{2+}–As^{3+} axial bond (Co–As = 2.51 Å) and nearly square-planar CoO_4. Owing to the high-spin character of the Co^{2+} ion, the interaction of the filled d_{z2} orbital of Co^{2+} with the filled lone-pair orbital of As^{3+} becomes a two-orbital three-electron stabilizing interaction, hence leading to the direct Co–As bond. BVS analysis indicates that the bond valence of the Co–As bond is about 0.33, which is reproduced by using $r_0 = 2.13$ for the Co^{2+}–As^{3+} bond. $BaCoAs_2O_5$ is expected to open a wide field of investigation for exotic magnetic oxides.

Experimental Section

Synthesis: In Ref. [25], we had mentioned the possibility of growing $BaCo^{2+}{}_2(As^{3+}{}_3O_6)_2{\cdot}(H_2O)_2$, a rare case of a Co^{2+}/As^{3+} oxide, by using a water/hydrazine solution. Similarly, the new $BaCo^{2+}As^{3+}{}_2O_5$ compound was obtained from $BaCO_3$, $CoCl_2$, and As_2O_3 (7:3.5:10.5 mmol) mixed in ca. 10 mL of distilled water. Hydrazine (2 mL/85 %) was used as a reducing agent. The mixture was then poured into a Teflon-lined autoclave, heated to 493 K for 72 h, and slowly cooled down to room temperature over 200 h. Blue needles of typically ca. $100 \times 20 \times 20\ \mu m^3$ were selected from the product. A sample made up of hand-selected single crystals has been used for further measurements. We note reproducibility difficulties in the preparation of the title compound.

XRD: Diffraction data were collected using a DUO-Bruker SMART apex diffractometer ($\lambda = Mo_{K\alpha}$). Intensities were extracted and corrected using the SAINT program.[28] Multi-scan absorption corrections were applied using the SADABS program.[29] The crystal structure refinements were performed using the JANA 2006 program.[30]

Magnetic susceptibility and magnetization measurements: Typical measurements were performed using the ZFC and FC procedures under a 0.1 T field with a MPMS Squid (Quantum Design). Magnetization measurements were carried out at 2 K.

EPR: X-band EPR experiments were carried out with a Bruker ELEXYS E580E spectrometer. Microwave power and modulation amplitude were 7.5 mW and 5 G, respectively.

DFT calculations: Spin polarized DFT calculations were performed using the Vienna ab initio Simulation Package (VASP)[31] with the generalized gradient approximation (GGA) for electron exchange and correlation corrections using the Perdew–Wang[32] functional and the frozen core projected wave vector method.[33] A plane wave energy cutoff energy of 400 eV, a total energy convergence threshold of 10^{-6}, and 102 k points in the irreducible Brillouin zone were used. The GGA plus on-site repulsion (GGA + U) method with effective $U = 3$ eV was also employed to account for the strong electron correlation associated with the 3d electrons on the Co atoms. The ELF and the density of states of O and As atoms are from the GGA-only calculations.

Received: December 24, 2013
Published online: February 12, 2014

Keywords: arsenites · cobalt · electronic structure · molecular modeling · solid-state structures

[1] A. Walsh, D. J. Payne, R. G. Egdell, G. W. Watson, *Chem. Soc. Rev.* **2011**, *40*, 4455.
[2] A. Walsh, G. W. Watson, D. J. Payne, R. G. Edgell, J. H. Guo, P. A. Glans, T. Learmonth, K. E. Smith, *Phys. Rev. B* **2006**, *73*, 235104.
[3] A. Walsh, Y. Yan, M. N. Huda, M. M. Al-Jassim, S.-H. Wei, *Chem. Mater.* **2009**, *21*, 547–551.
[4] C. E. Mohn, S. Stølen, *Phys. Rev. B* **2011**, *83*, 014103.
[5] R. Seshadri, N. A. Hill, *Chem. Mater.* **2001**, *13*, 2892–2899.
[6] L. F. Pašteka, T. Rajský, M. Urban, *J. Phys. Chem. A* **2013**, *117*, 4472–4485.
[7] T. Araki, P. B. Moore, *Am. Mineral.* **1981**, *66*, 1263–1273.
[8] D. D. F. Pertlik, *Mineral. Petrol.* **1987**, *36*, 85–92.
[9] F. Pertlik, *Monatsh. Chem.* **1986**, *117*, 1257–1261.
[10] Z. Yang, G. Giester, K. Ding, E. Tillmanns, *Eur. J. Mineral.* **2011**, *23*, 63–71.
[11] T. A. Albright, J. K. Burdett, M. H. Whangbo, *Orbital Interactions in Chemistry, 2nd ed.*, John Wiley & sons, Inc. Hoboken, New Jersey, 2013.
[12] D. Dai, J. Ren, W. Liang, M. H. Whangbo, *SAMOA (Structure and Molecular Orbital Analyzer) Program Package*, http://chvamw.chem. Ncsu.edu/, **2002**.
[13] R. Hoffmann, *J. Chem. Phys.* **2004**, *120-121*, 1397–1412.
[14] W. J. Zhu, P. H. Hor, A. J. Jacobson, G. Crisci, T. A. Albright, S.-H. Wang, T. Vogt, *J. Am. Chem. Soc.* **1997**, *119*, 12398–12399.
[15] C. S. Knee, M. T. Weller, *J. Solid State Chem.* **2002**, *168*, 1–4.
[16] C. F. Smura, D. R. Parker, M. Zbiri, M. R. Johnson, Z. A. Gál, S. J. Clarke, *J. Am. Chem. Soc.* **2011**, *133*, 2691–2705.
[17] D. Dai, H. Xiang, M.-H. Whangbo, *J. Comput. Chem.* **2008**, *29*, 2187–2209.
[18] H. Xiang, C. Lee, H.-J. Koo, X. Gong, M.-H. Whangbo, *Dalton Trans.* **2012**, *41*, 823–853.
[19] A. Abragam, M. H. L. Pryce, *Proc. R. Soc. London Ser. A* **1951**, *206*, 173.
[20] "Spectral-Structural Correlations in High-Spin Cobalt(II) Complexes": L. Banci, A. Bencini, C. Benelli, D. Gatteschi C. Zanchini, *Structure and Bonding 52*, Springer, Berlin/Heidelberg, **1982**.
[21] K. Yamada, M. Matsuda, Y. Endoh, B. Keimer, R. J. Birgeneau, S. Onodera, J. Mizusaki, T. Matsuura, G. Shirane, *Phys. Rev. B* **1989**, *39*, 2336–2343.
[22] O. H. Hansteen, H. Fjellvåg, B. C. Hauback, *J. Solid State Chem.* **1998**, *141*, 411–417.
[23] O. H. Hansteen, H. Fjellvåg*, B. C. Hauback, *J. Mater. Chem.* **1998**, *8*, 2089–2093.
[24] L. P. Regnault, P. Burlet, J. Rossat-Mignod, *Phys. B + C* **1977**, *86*, 660–662.
[25] R. David, H. Kabbour, S. Colis, O. Mentré, *Inorg. Chem.* **2013**, *52*, 13742–13750.
[26] N. E. Brese, M. O'Keeffe, *Acta Crystallogr. Sect. B* **1991**, *47*, 192–197.
[27] B. Silvi, A. Savin, *Nature* **1994**, *371*, 683–686.
[28] *SAINT*: *Area-Detector Integration Software*, Siemens Industrial Automation, Inc.: Madison, WI, **1995**.
[29] *SADABS*: *Area-Detector Absorption Correction*, Siemens Industrial Automation, Inc.: Madison, WI, **1996**.
[30] V. Petricek, M. Dusek, L. Palatinus, JANA2000 Crystallogr. Comput. Syst. Inst. Phys. Praha Czech Repub. **2000**.
[31] G. Kresse, J. Furthmüller, *Vienna Ab-Initio Simulation Package (VASP)*, Institut Für Materialphysik: Vienna (http://cms.mpi.univie.ac.at/vasp), **2004**.
[32] J. P. Perdew, Y. Wang, *Phys. Rev. B* **1992**, *45*, 13244–13249.
[33] G. Kresse, D. Joubert, *Phys. Rev. B* **1999**, *59*, 1758–1775.

